

Spectral Power Variation Separates Oscillatory from Non-Oscillatory Stochastic Neural Dynamics

Richard Gao (rigao@ucsd.edu)

Department of Cognitive Science, University of California, San Diego

Lauren Liao (ldliao@ucsd.edu)

Department of Mathematics, University of California, San Diego

Bradley Voytek (bvoytek@ucsd.edu)

Department of Cognitive Science & Neurosciences Graduate Program, University of California, San Diego
9500 Gilman Drive, La Jolla, CA 92093, USA

Abstract

Oscillatory brain activity observed in neural field potentials has been widely used to index behavior, cognition, and disease. There is emerging evidence, however, that oscillations can exist in different modes, such as sustained versus bursting, that have different physiological origins and different behavioral relevance. Additionally, there exist other, non-oscillatory components in the field potential that can obscure or be mistaken for oscillations, especially in the mean power spectral density (PSD). One such component is the aperiodic signal that gives rise to the $1/f$ power law background in the field potential PSD, which has been proposed to reflect synaptic potentials induced by Poisson population spiking. It remains an ongoing challenge to consistently define, operationalize, and isolate oscillatory and non-oscillatory neural dynamics. In this work, we begin with a model of the field potential as a superposition of the aperiodic (Poisson) component and oscillatory components. We use two measures – spectral coefficient of variation (SCV) and deviation from noise power distribution – that are able to separate these components in simulation. Finally, we demonstrate the existence and separation of these components in a range of experimental data, focusing on human electrocorticography during movement in this paper.

Keywords: Poisson population; oscillation; high gamma; LFP; ECoG

Background

One of the key observations in systems neuroscience is that cortical neurons in spontaneous and in-vivo conditions often fire action potentials in a seemingly stochastic manner, where the distribution of interspike interval (ISI) approaches an exponential distribution, similar to events drawn from a Poisson point process (e.g., (Softky & Koch, 1993), but see (Maimon & Assad, 2009) for observed exceptions). Extrapolated to an entire population, this dynamical regime has been coined the asynchronous irregular state (Brunel, 2000). When recurrently connected, and balanced between excitation and inhibition (E-I), the asynchronous population

activity in turn generates a baseline stochastic perturbation (neuronal noise) in an individual cell’s membrane voltage. This seemingly circular but self-consistent mechanism enables the single cell to emit action potentials in a Poisson-like fashion, which has also been argued to be advantageous for circuit computation (e.g., van Vreeswijk & Sompolinsky, 1996, and Zerlaut & Destexhe, 2017 for recent review). Based on this line of work, there has been a symbiotic convergence of systems and computational neuroscience: the E-I balanced network provides a robust and rich dynamical system theorized to underlie a wide range of brain functions. This class of neuronal dynamics, however, has not been studied in detail in human cognitive neuroscience until very recently, likely due to the lack of access to single and multi-unit recordings in humans.

In addition to the asynchronous state, individual neurons and neural populations also exhibit synchronous, oscillatory dynamics. These electrophysiological features can be very strong, dominating the signal and making them easy to record and measure. The asynchronous and synchronous states can coexist simultaneously in different neural populations, and underlie two ends of a spectrum: previously, asynchronous population activity has been related to desynchronization (of alpha and beta oscillations) in the EEG, though this characterization lacks detail. Furthermore, the “desynchronized state” is sometimes held to be synonymous with low-amplitude, high-frequency oscillations - in particular, the 40 Hz gamma oscillation - which is erroneous as gamma oscillation is an entirely different network state reflecting local synchrony (Ahmed & Cash, 2013).

More recently, observations from simultaneous single unit and field potential recordings (local field potential, LFP, and electrocorticography, ECoG) revealed that single unit firing rate is correlated with high-frequency (high-gamma) and broadband power of field potential in nearby regions, where the canonical $1/f$ power spectral density (PSD) shifts up or down, either in frequencies above 100 Hz (Mukamel et al., 2005), or in a broadband manner (Manning, Jacobs, Fried, & Kahana, 2009). These observations are modeled as additive or multiplicative gains in the firing rate of a Poisson population, and can be dissected with more sophisticated analytical tools, such as PCA decomposition of the spectrogram (Miller, Zanos, Fetz, Nijs, & Ojemann, 2009) or

parameterization of the PSD (Haller et al., 2018). Based on the Poisson population model, high-gamma and broadband power have been used in recent ECoG studies to infer firing rate changes, as well as other variables like “neural noise” in aging and E-I balance (Gao, Peterson, & Voytek, 2017; Voytek et al., 2015). These interpretations are not yet well supported, however, for two reasons. First, the synaptic-filtered heterogeneous-rate Poisson population model was only shown to capture the shape of the 1/f PSD and changes in mean power, but not any other higher-order statistics. Second, other brain dynamics, such as oscillations, neuronal avalanches, or ERPs, often contribute significantly to the signal power and, as a result, decoupling these processes from asynchronous population dynamics using the mean power spectral density alone remains a contemporary challenge (though various existing tools have seen success at doing so see Haller et al., 2018; Wen & Liu, 2016). For instance, in the high-frequency range (~100 Hz), there is ongoing debate about whether neuronal excitation manifests as an increase in wideband oscillations or asynchronous noise signal, or both (Hermes, Miller, Wandell, & Winawer, 2015).

In this work, we begin by modeling the baseline (“noise”) field potential as synaptic potentials induced by stationary and homogeneous Poisson population firing. We derive analytically, and demonstrate with simulation, that while mean spectral power decreases with increasing frequency (1/f power law), power at any single frequency follows an exponential distribution (across time) parameterized by the mean power, such that the standard deviation is equal to the mean. We leverage two metrics to identify stationary stochastic dynamics, and deviations from it, in field potentials over time: 1) spectral coefficient of variation (SCV), and 2) Kolmogorov-Smirnov test statistic against the null exponential distribution (KS-stat). We show that both metrics are sensitive to simulated oscillatory signals added to the noise LFP. Finally, using a variety of publically available datasets (resting and task for rodent LFP, monkey ECoG and EEG, and human ECoG and EEG), we demonstrate:

1. The existence of a “noise band” between 30-70 Hz that typically follows the null exponential distribution regardless of brain region, task, or species.
2. The superposition of oscillatory and other types of frequency-dependent dynamics onto the baseline power distribution of the aperiodic signal in other frequencies (such as the 10-25 Hz beta range during movement).
3. The ability to distinguish between bursting vs. sustained oscillations, as well as between narrowband vs. broadband processes, based on first principle derivation, rather than heuristically examining the average power spectrum.
4. Evidence for rate-varying stochastic neural populations that activate in a task-dependent manner, resulting in a shift in mean power but maintaining a noise-like distribution.

This work makes contributions towards model-driven analysis of neural field potentials, particularly oscillatory and high-gamma components, in addition to establishing theoretical advances in linking asynchronous population dynamics to meso- and macroscale field potential signals that are more widely accessible in cognitive neuroscience. Due to space constraint, the rest of the paper will present an overview of the method, as well as key findings from simulated and human ECoG data. All simulation and analysis code can be found at online:

<https://github.com/voytekresearch/spectralCV>

Methods

Poisson Population & Oscillation Simulation

We start with a generative model of the LFP as filtered Poisson population firing, i.e. white noise convolved with an exponentially rising and decaying synaptic response. This model of mesoscale field potential was previously used in (Miller et al., 2009), and is similar to a 1D random walk with memory (i.e. Ornstein Uhlenbeck process) previously used to model intracellular fluctuations during the high-conductance state (Destexhe, Rudolph, Fellous, & Sejnowski, 2001). Two kinds of oscillatory signals were added to the 2-minute long baseline noise LFP simulation: one stationary-amplitude and one bursting, with specified on-off transition probabilities.

Windowed Fourier Analysis

For both simulated and experimental data, signal spectrograms are computed using short time Fourier transforms (STFT) with non-overlapping or partially overlapping sliding windows such that sequential power estimates remain independent. In trialed analyses, the spectrogram is built by concatenating single-window FFTs computed from data immediately prior to (and after) trial onset. The sequence of spectral power at frequency f over the entirety of the signal forms the power distribution at f Hz, $P(f)$. The mean of the distribution is, by definition, the power spectral density at frequency f as computed using Welch’s method. Mean power ($1/\lambda$) is used to parameterize the null exponential distribution, to which we compare the empirical distribution to using the Kolmogorov-Smirnov test (see results for derivation of null distribution). Additionally, we compute the spectral coefficient of variation (SCV, standard deviation over mean), which equals 1 for the exponential distribution.

Results

Derivation of Null Spectral Power Distribution

When white noise is Fourier transformed, the Fourier coefficient at any frequency is a complex random variable drawn from a 2D normal distribution, with mean zero and variance proportional to the total signal power within the FFT window (Parseval’s theorem). The squared vector norm (spectral power) is then a sum of two independently distributed normal variables with equal variance, i.e., P

follows the exponential distribution $P(x) \sim \lambda \exp(-\lambda x)$, where λ fully parameterizes the exponential distribution and $1/\lambda$ represents the mean power at that frequency. Convolution with white noise with the synaptic response filter is equivalent to scaling λ at each frequency, but does not affect the shape of the distributions. This means that even though power varies as a function of frequency, following a power law decay, power for each frequency remains exponentially distributed, and thus the signature of aperiodic activity should in theory be identifiable at any frequency when not obscured by narrowband components with a higher amplitude, e.g., an oscillation. We refer to this filtered noise signal as baseline noise LFP.

Simulation and Analysis of Poisson Population Field Potential with Oscillations

In the simulation experiment, a stationary oscillation (4 Hz) and a bursting oscillation (23 Hz) were added to the baseline noise LFP. We performed the simulation 50 times (trials) for 120 seconds each, and computed the PSD, SCV, and KS test p-value (Figure 1., each trace is a trial; example time series in Fig. 1a). We observe two oscillatory bumps above the $1/f$ power law background from the aperiodic component in the PSD (Fig.1b), though the background spectrum partially obscures the bandwidth and amplitude of the oscillations.

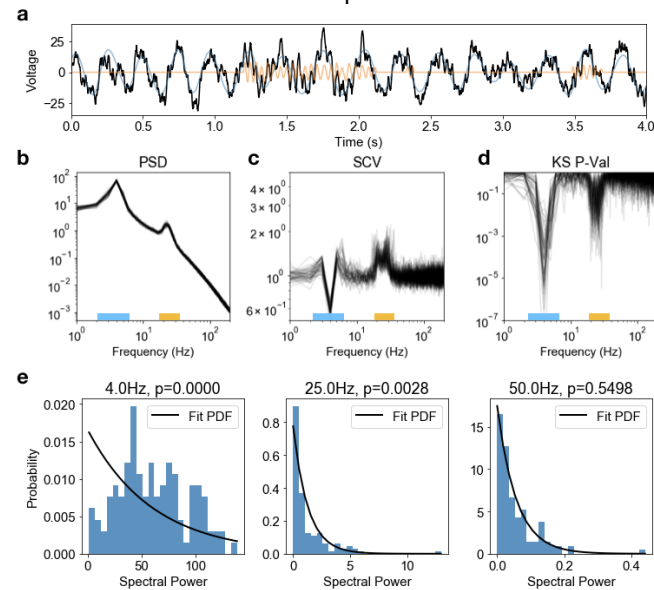


Figure 1: Analysis of simulated noise LFP with stationary and bursting oscillations. a) Example simulated LFP overlaid with stationary (blue) and bursting (orange) oscillation. b-d) power, power variation, and noise deviation separating aperiodic and oscillatory components in the signal. e) power distribution across time at 4, 25, and 50Hz showing deviation and conformity to the null exponential distribution.

Both the SCV and KS tests, however, show clearer discrimination between non-oscillatory and oscillatory regions in the spectrum. In Fig.1c, SCV is ~ 1.0 everywhere

except at the oscillatory frequencies, consistent with the above derivations. SCV at 4 Hz is < 1.0 in all trials, since a stationary (ongoing) oscillation has little variation in power compared to its mean. In contrast, the bursting oscillation (20-27 Hz), which has high variability in power compared to the mean, effectively has a bimodal power distribution, toggling between the aperiodic and oscillatory state, thus pushing SCV to > 1.0 . KS test p-values show that the empirical power distributions are not significantly different (at $p_{\text{thresh}}=0.01$) from the null (exponential) distributions except at frequencies where oscillations exist (Fig.1c).

Looking at power distributions from a single trial (Fig.1e), we observe that the stationary oscillation at 4 Hz (left) results in a more symmetrical distribution due to its well-defined oscillatory nature, while the bursting oscillation at 25 Hz (middle) elongates the right-tail, representing time periods where bursting is present (p-values in title denote KS test against exponential null). Power distribution at 50 Hz follows the predicted null closely. These results demonstrate the utility of higher-order moments in differentiating stationary and bursting oscillatory dynamics from the stochastic Poisson population dynamics, as well as from each other.

Movement-Dependent Activation of Oscillatory Beta and Stochastic High-Gamma

We analyze previously published human ECoG data, where patients undergoing epilepsy monitoring participate in a finger-flexion task (Miller et al., 2009). Between periods of resting, cues are presented to the participants to repeatedly move a single digit, and accelerometer data is captured as well. In addition to continuous sliding-window analysis over the entire recording (“whole” condition), trialed analysis was performed by applying windowed FFT to 1-second of data immediately preceding and following onset of movement, and trial-concatenated to form the “pre” or “move” condition, respectively. Figure 2 presents data from M1 electrode of one subject (148 completed trials). Comparing mean PSDs of pre and move states (Fig. 2a), we see previously reported movement-related decrease in oscillatory beta (or mu, 10-20 Hz) power and increase in high gamma (70-100 Hz) power. However, SCV and KS test reveal two novel observations.

First, during both pre and move conditions, high gamma frequencies have SCV close to 1 and are not significantly different from the null distribution, while whole-recording analysis shows a significant deviation from the null (Fig. 2b,c). This suggests that high gamma frequencies in M1 for this experiment reflects Poisson-like populations that increase in rate during task-demand, but remain stochastic in nature during both conditions. This is confirmed in Fig. 2d, where power around 80 Hz for pre and move conditions closely follow the fitted exponential distributions, but differ in mean power. Second, while there is a prominent burst-like beta/mu oscillation during pre-movement periods, the oscillation disappears during movement, as shown by the flat SCV and KS p-value plots for movement period. This is not simply a decrease in power of a sustained oscillation, but rather the halting of an oscillatory process that is usually over

and above the background asynchronous population dynamics during rest, i.e. a bursting oscillator.

As a final measure, Fig. 2e plots pre vs. move power of every trial in 3 different frequency bands. While there is a clear shift in beta and high-gamma power (in opposite directions), reflecting an overall decrease and increase respectively, pre and move period power for a single trial are largely independent. Taken altogether, these observations support the interpretation that high-gamma power is in effective randomly drawn from two exponential distributions parameterized with different means, representative of an increase in Poisson population firing rate. Similarly, when the typically high-amplitude oscillatory process at beta frequency is removed, it exposes the underlying signature of a baseline stochastic population dynamics – but at a much lower frequency. Thus, we argue that the stochastic Poisson population dynamics should be reflected in the broadband field potential recording, though only in the absence of stronger and structured (narrowband) dynamics.

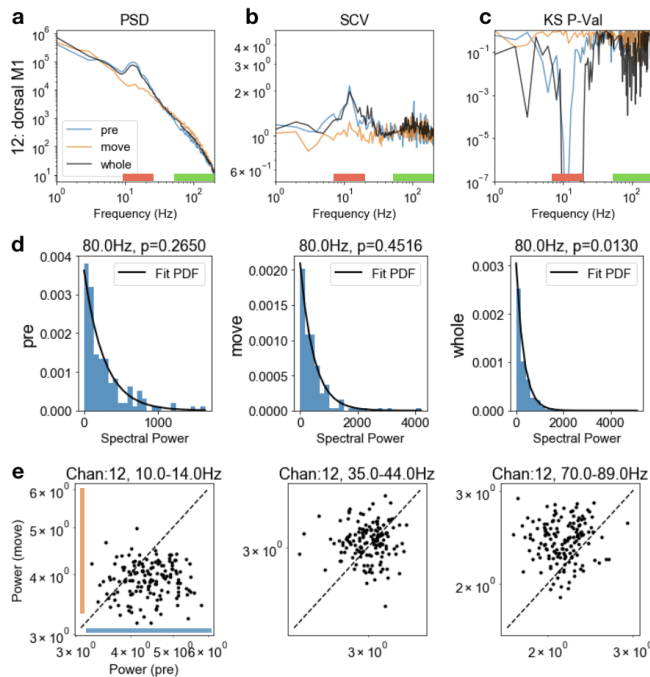


Figure 2: Spectral representation of human ECoG during motor task. a-c) power, power variation, and noise deviation separating aperiodic and oscillatory components in the signal. Beta oscillation and high-gamma signal is highlighted in red and green, respectively. In particular, note the flat SCV and noise deviation in the orange trace in b-c). d) Power distribution at 80Hz for pre-movement, movement, and whole-recording analysis. e) Pre-movement and movement power in a trial in beta, “noise”, and high gamma frequencies are independent.

References

- Ahmed, O. J., & Cash, S. S. (2013). Finding synchrony in the desynchronized EEG: the history and interpretation of gamma rhythms. *Frontiers in Integrative Neuroscience*, 7, 58.
- Brunel, N. (2000). Dynamics of sparsely connected networks of excitatory and inhibitory spiking neurons. *Journal of Computational Neuroscience*, 8(3), 183–208.
- Destexhe, A., Rudolph, M., Fellous, J. M., & Sejnowski, T. J. (2001). Fluctuating synaptic conductances recreate in vivo-like activity in neocortical neurons. *Neuroscience*, 107(1), 13–24.
- Gao, R., Peterson, E. J., & Voytek, B. (2017). Inferring synaptic excitation/inhibition balance from field potentials. *NeuroImage*, 158, 70–78.
- Haller, M., Donoghue, T., Peterson, E., Varma, P., Sebastian, P., Gao, R., et al. (2018). Parameterizing neural power spectra. *bioRxiv*
- Hermes, D., Miller, K. J., Wandell, B. A., & Winawer, J. (2015). Stimulus Dependence of Gamma Oscillations in Human Visual Cortex. *Cerebral Cortex*, 25(9), 2951–2959.
- Maimon, G., & Assad, J. A. (2009). Beyond Poisson: Increased Spike-Time Regularity across Primate Parietal Cortex. *Neuron*, 62(3), 426–440.
- Manning, J. R., Jacobs, J., Fried, I., & Kahana, M. J. (2009). Broadband shifts in local field potential power spectra are correlated with single-neuron spiking in humans. *Journal of Neuroscience*, 29(43), 13613–13620.
- Miller, K. J., Zanos, S., Fetz, E. E., Nijs, den, M., & Ojemann, J. G. (2009). Decoupling the Cortical Power Spectrum Reveals Real-Time Representation of Individual Finger Movements in Humans. *Journal of Neuroscience*, 29(10), 3132–3137.
- Mukamel, R., Gelbard, H., Arieli, A., Hasson, U., Fried, I., & Malach, R. (2005). Coupling between neuronal firing, field potentials, and fMRI in human auditory cortex. *Science (New York, N.Y.)*, 309(5736), 951–954.
- Softky, W. R., & Koch, C. (1993). The highly irregular firing of cortical cells is inconsistent with temporal integration of random EPSPs. *Journal of Neuroscience*, 13(1), 334–350.
- van Vreeswijk, C., & Sompolinsky, H. (1996). Chaos in neuronal networks with balanced excitatory and inhibitory activity. *Science (New York, N.Y.)*, 274(5293), 1724–1726.
- Voytek, B., Kramer, M. A., Case, J., Lepage, K. Q., Tempesta, Z. R., Knight, R. T., & Gazzaley, A. (2015). Age-Related Changes in 1/f Neural Electrophysiological Noise. *Journal of Neuroscience*, 35(38), 13257–13265.
- Wen, H., & Liu, Z. (2016). Separating Fractal and Oscillatory Components in the Power Spectrum of Neurophysiological Signal. *Brain Topography*, 29(1), 13–26.
- Zerlaut, Y., & Destexhe, A. (2017). Enhanced Responsiveness and Low-Level Awareness in Stochastic Network States. *Neuron*, 94(5), 1002–1009.